

Towards Modeling Human Motor Learning Dynamics in High-Dimensional Spaces

Ankur Kamboj, Rajiv Ranganathan, Xiaobo Tan, and Vaibhav Srivastava

Abstract—Designing effective rehabilitation strategies for upper extremities, particularly hands and fingers, warrants the need for a computational model of human motor learning. The presence of large degrees of freedom (DoFs) available in these systems makes it difficult to balance the trade-off between learning the full dexterity and accomplishing manipulation goals. The motor learning literature argues that humans use motor synergies to reduce the dimension of control space. Using the low-dimensional space spanned by these synergies, we develop a computational model based on the internal model theory of motor control. We analyze the proposed model in terms of its convergence properties and fit it to the data collected from human experiments. We compare the performance of the fitted model to the experimental data and show that it captures human motor learning behavior well.

I. INTRODUCTION

Motor impairments after a neurological injury such as stroke are one of the leading causes of disability in the United States [1]. Impairments of upper extremities in particular, including hand and finger function, are extremely common, with 75% of stroke survivors facing difficulties performing daily activities [2], [3]. Critically, impairments after stroke not only include muscle and joint-specific deficits such as weakness and changes in the kinematic workspace [4], but also coordination deficits such as reduced independent joint control and impairments in finger individuation and enslaving [5], [6]. Thus, understanding how to address these coordination deficits is critical for improving movement rehabilitation.

A key step in addressing these coordination deficits in the upper extremity and promoting rehabilitation is the development of a computational model of learning that takes place in human motor systems [7]. These motor systems involve large DoFs, for example, the hand alone has over 25 joints and 30 muscles which gives rise to the incredible dexterity that we possess when grasping and manipulating objects. A key challenge to motor learning in such high-dimensional spaces is to balance the exploration required to learn full dexterity induced by the high DoFs and learning enough dexterity to generate desired motion. The motor learning literature has argued that the human nervous system uses a small number of *motor synergies* to control the high-DoF body motor systems [8]. Santello *et al.* [9] concluded that two

principal postural synergies accounted for more than 80% of the postural data collected from various grasp postures, suggesting that most of the grasping postures can be explained by just two underlying motor synergies, a substantial reduction from the 15 DoF data that they recorded. We build on this idea of motor synergies to develop a dynamical model of human motor learning (HML).

The need for models of human motor learning systems for physical as well as robotic rehabilitation has been outlined in [7]. While several learning mechanisms have been proposed for human motor learning processes [10], it has mostly been viewed in literature as adaptation in motor tasks, and consequently, several computational models of human motor learning have been rooted in adaptive control theory. For example, Shadmehr *et al.* [11] proposed the idea of dynamic internal model in human motor learning that adapts to the changed limb dynamics because of a force field imposed on the hand. Similarly, Zhou *et al.* [12] leveraged iterative model reference adaptive control to model human learning through repetitive tasks. However, most of these works only deal with motor learning in relatively low-dimensional spaces.

Pierella *et al.* [13] study motor learning of a novel task in high DoF motor systems where multiple solutions are available. They develop a dynamic model of motor learning that relies on the formation of internal models only at the end of a trial. We develop similar models for motor learning tasks studied in this paper. This work is distinct from [13] in two key aspects: (a) the motor learning tasks studied in this paper involve higher DoFs, which require the use of synergies for efficient modeling, and (b) our setup deals with continuous feedback, which leads to faster learning but presents modeling and estimation challenges.

In this paper, we develop a computational model of human motor learning in high-dimensional spaces using the context of learning novel coordinated hand finger joints movements. Our model is based on the internal model theory of motor control [14] and leverages the idea of motor synergies for efficient learning using low-dimensional representations. Based on the evidence in the motor learning literature [15], the model comprises a fast forward learning dynamics and a slow inverse learning dynamics. We analyze the model using techniques from adaptive control theory and singular perturbation analysis, and establish its convergence properties. Finally, we fit the proposed model to experimental data, and compare the fitted model with the experimental data to show that it captures human motor learning behavior effectively.

The rest of the paper is organized as follows. Section II

This work has been supported by NSF Award CMMI-1940950.

A. Kamboj, X. Tan, and V. Srivastava are with the Department of Electrical and Computer Engineering, Michigan State University, East Lansing, MI 48823 USA. {ankurank, xbtan, vaibhav}@msu.edu.

R. Ranganathan is with the Department of Kinesiology, Michigan State University, East Lansing, MI 48823 USA. rrangana@msu.edu.

outlines the experimental setup that we leverage to build our motor learning model as well as some data preprocessing techniques we adopted in the paper. Section III describes the proposed computational model and is followed by its convergence analysis in Section IV. In Section V, we fit our model to experimental data and compare its performance with the human data. We conclude and provide some future directions in Section VI.

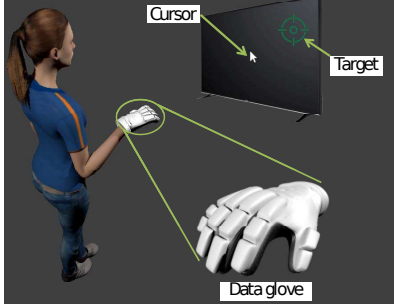


Fig. 1: Artistic rendering of the experimental setup with the subject wearing the data glove.

II. BACKGROUND

In this section, we present the experimental paradigm leveraged in this paper to model human motor learning in high-dimensional spaces. We also discuss techniques for preprocessing of data collected from these experiments.

A. Learning Coordinated Finger-joints Movements: Experimental Setup

Motor (re)-learning is central to the rehabilitation of individuals with hand and finger impairments and/or paresis. It is believed that the mechanisms underlying re-learning during rehabilitation are similar to mechanisms underlying learning of a novel task by healthy subjects. We focus on the motor learning experiment presented in [16] wherein healthy subjects learn a novel motor task. Each subject wears a data glove (CyberGlove, Immersion Technologies, Inc.), which records the movement of each of the 19 finger joints. A human machine interface (HMI) uses a matrix to project the 19-dimensional finger movements onto the movement of a cursor on a 2-D computer screen; see Fig. 1. Specifically, the HMI projects the vector of finger joint velocities $\mathbf{u} \in \mathbb{R}^m$ to cursor velocity $\dot{\mathbf{x}} \in \mathbb{R}^n$ using a matrix $C \in \mathbb{R}^{n \times m}$ such that

$$\dot{\mathbf{x}} = C\mathbf{u}. \quad (1)$$

Here, $n = 2$ and $m = 19$. The subjects need to move the cursor to a target point, and a new target point is prescribed once the current target is reached. To this end, subjects need to learn coordinated finger joint movements that are consistent with the (unknown) projection matrix C . This experiment naturally involves motor learning in high-dimensional spaces, with the output being in the low-dimensional screen space. Each subject participated in eight sessions, each comprised of 60 trials. In each trial, the sequence of target points were randomly selected from 4 points located at $(0.5, 4.5), (2.5, 0.5), (2.5, 2.5), (4.5, 4.5)$ units on

the screen. Due to the large nullspace of C , this task is redundant in the sense that a desired cursor movement can be achieved with multiple synergistic motions of finger joints. However, to what extent subjects learn the optimal (minimum energy) synergistic motion is of interest.

B. Preprocessing Finger-joints Movement Data

The data glove records finger joints data, which is used for updating cursor positions. However, mapping (1) is described in terms of joint and cursor velocities. We adopt a standard technique from adaptive control that allows us to re-write (1) using filtered joint and cursor position data [17]. We write the system dynamics (1) using a mixed frequency-time notation as $s\mathbf{x} = C\mathbf{u}$, where s denotes the Laplace variable. Dividing both sides by $s + a$, for some $a > 0$ gives us

$$\begin{aligned} \frac{s}{s + a}\mathbf{x} &= \frac{1}{s + a}C\mathbf{u}, \\ -\frac{a}{s + a}\mathbf{x} + \mathbf{x} &= \frac{1}{s + a}C\mathbf{u}. \end{aligned} \quad (2)$$

Define the signals $\chi = \mathbf{x}/(s + a)$, and $\delta\mathbf{u} = \mathbf{u}/(s + a)$, or $\dot{\chi} = -a\chi + \mathbf{x}$ and $\delta\mathbf{u} = -a\delta\mathbf{u} + \mathbf{u}$, i.e., χ and $\delta\mathbf{u}$ are filtered cursor position and joint velocity, respectively. Then, in the time-domain Eq. (2) reduces to

$$-\mathbf{a}\chi + \mathbf{x} = C\delta\mathbf{u}.$$

Defining $\delta\mathbf{x} = -\mathbf{a}\chi + \mathbf{x}$, we get the system equation as

$$\delta\mathbf{x} = C\delta\mathbf{u}. \quad (3)$$

$\delta\mathbf{x}$ and $\delta\mathbf{u}$ are termed *filtered cursor velocity*, and *filtered finger joints velocities*, respectively.

III. ADAPTIVE CONTROL-BASED HML COMPUTATIONAL MODEL

Motor learning literature [8], [9] suggests that humans control the high DoF body motor systems using a small number of coordinated joint movement patterns called synergies. For example, four synergies spanned more than 80% of the the finger joints configurations required to generate the American Sign Language (ASL) Alphabet [18], [19]. We assume that the mapping matrix $C = W\Phi$, where $\Phi \in \mathbb{R}^{h \times m}$ is a matrix of h basic synergies underlying coordinated human finger motions, and $W \in \mathbb{R}^{n \times h}$ are the contributions (weights) of these synergies during a particular hand motion. We assume that Φ is an orthonormal matrix, i.e., the synergies contributing to the hand motions lie in orthogonal spaces. We further assume these synergies to be known (see Section V-A for details). While our motor learning model is in the original high-dimensional space, these synergies reduce the size of the learning space and enable efficient learning by reducing the amount of desired exploration.

It is believed that motor learning in humans involves the formation of internal models [11], including models for forward and inverse learning. The forward model predicts the outcomes of motor actions (hand joint movements), whereas the inverse model predicts the motor actions required to generate certain outcomes. In this section, we adopt techniques

from adaptive control theory to develop models of forward and inverse human motor learning dynamics.

A. Adaptive Control-based Model of Forward Learning

In the context of the experimental setup described in Section II, forward learning entails learning the forward HMI mapping matrix, i.e., the mapping matrix C . Suppose that at time t , human subject's (implicit) estimate of matrix C is $\hat{C}(t)$. Correspondingly, the estimated filtered cursor velocity is $\hat{\delta}\mathbf{x} \in \mathbb{R}^n$ for filtered finger joints velocities $\delta\mathbf{u} \in \mathbb{R}^m$ is

$$\hat{\delta}\mathbf{x} = \hat{C}\delta\mathbf{u}, \quad (4)$$

where $\hat{C} = \hat{W}\Phi$, and $\hat{W}(t) \in \mathcal{W} \subseteq \mathbb{R}^{n \times h}$ is the parameter estimate matrix, which determines the weight the human subject assigns to each synergy. It follows from (3) and (4) that the estimation error

$$\epsilon = \delta\mathbf{x} - \hat{\delta}\mathbf{x} = -\tilde{W}\Phi\delta\mathbf{u}, \quad (5)$$

where $\tilde{W}(t) = \hat{W}(t) - W \in \mathbb{R}^{n \times h}$ is the parameter estimation error.

It is well known in adaptive control literature that the gradient descent for \hat{W} on $\frac{1}{2}\|\epsilon\|^2$ leads to estimation error converging to zero. Accordingly, we select

$$\dot{\hat{W}} = -\gamma \nabla_{\hat{W}} \frac{1}{2}\|\epsilon\|^2 = \gamma\epsilon\delta\mathbf{u}^\top\Phi^\top, \quad (6)$$

where $\gamma > 0$ is the forward learning rate, $\dot{\hat{W}} \in \mathcal{E}_W \subseteq \mathbb{R}^{n \times h}$, and $(\cdot)^\top$ represents the transpose. We posit (6), with γ as a tunable parameter, as a model for human forward learning dynamics. This model is consistent with the error-based human motor learning paradigm and similar models have been used in literature; see e.g., [13], [20].

B. Adaptive Control-based Model of Inverse Learning Dynamics

The inverse learning concerns identifying coordinated finger joint movements that drive the cursor to a desired position. If the mapping matrix C is known, then the following proportional control will drive the cursor to the desired position x^{des}

$$\mathbf{u} = k_P C^\dagger (x^{\text{des}} - \mathbf{x}) = k_P C^\dagger \mathbf{e}_x, \quad (7)$$

where C^\dagger is the pseudo-inverse of C , \mathbf{x} is the current cursor position, and $k_P > 0$ is the (scalar) proportional gain. We refer to the difference between the desired and current cursor position as the *Reaching Error (RE)* and denote it by \mathbf{e}_x .

Since mapping matrix C is not known, C^\dagger in (7) can be replaced by \hat{C}^\dagger , where \hat{C} is computed using forward learning model. It may not be reasonable to assume that humans can compute the pseudo-inverse of their implicit estimate \hat{C} . Therefore, we postulate that human subjects determine control input (7) through gradient-descent based learning. To this end, we let

$$\dot{\hat{\mathbf{u}}} = -\eta \nabla_{\hat{\mathbf{u}}} \left(\frac{1}{2} \|\dot{\hat{\mathbf{x}}} - k_P \mathbf{e}_x\|^2 + \frac{\mu}{2} \|\hat{\mathbf{u}}\|^2 \right),$$

where $\dot{\hat{\mathbf{u}}} \in \mathcal{E}_U \subseteq \mathbb{R}^m$, $\hat{\mathbf{u}} \in \mathcal{U} \subseteq \mathbb{R}^m$, and $\hat{\mathbf{x}}$ is the estimated cursor position based on subject's estimate of mapping matrix $\hat{C}(t)$. Here $\eta > 0$ is the inverse learning rate, and $\mu > 0$ is the regularizer weight. Note that this learning dynamics for $\hat{\mathbf{u}}$ minimizes the difference between the estimated and desired cursor velocity subject to regularization constraint for $\hat{\mathbf{u}}$. Upon simplification, these dynamics reduce to

$$\begin{aligned} \nabla_{\hat{\mathbf{u}}} & \left(\frac{1}{2} \|\dot{\hat{\mathbf{x}}} - k_P \mathbf{e}_x\|^2 + \frac{\mu}{2} \|\hat{\mathbf{u}}\|^2 \right) \\ &= \nabla_{\hat{\mathbf{u}}} \left(\frac{1}{2} \|\hat{C}\hat{\mathbf{u}} - k_P \mathbf{e}_x\|^2 + \frac{\mu}{2} \|\hat{\mathbf{u}}\|^2 \right), \\ &= \hat{C}^\top (\hat{C}\hat{\mathbf{u}} - k_P \mathbf{e}_x) + \mu\hat{\mathbf{u}}, \\ &= (\hat{C}^\top \hat{C} + \mu I) \hat{\mathbf{u}} - k_P \hat{C}^\top \mathbf{e}_x, \end{aligned} \quad (8)$$

which results in

$$\begin{aligned} \dot{\hat{\mathbf{u}}} &= -\eta \left((\hat{C}^\top \hat{C} + \mu I) \hat{\mathbf{u}} - k_P \hat{C}^\top \mathbf{e}_x \right), \\ &= -\eta \left((\Phi^\top \hat{W}^\top \hat{W}\Phi + \mu I) \hat{\mathbf{u}} - k_P \Phi^\top \hat{W}^\top \mathbf{e}_x \right). \end{aligned} \quad (9)$$

It should be noted that we do not anticipate that human subjects can explicitly compute RHS of (9). However, we assume that they can implicitly determine RHS of (9) by finding the direction of steepest descent for $\frac{1}{2} \|\dot{\hat{\mathbf{x}}} - k_P \mathbf{e}_x\|^2 + \frac{\mu}{2} \|\hat{\mathbf{u}}\|^2$. We posit (9), with η as a tunable parameter, as a model for human inverse learning dynamics. We refer to (6) and (9) together as the HML dynamics model.

IV. ANALYSIS OF THE ADAPTIVE CONTROL-BASED MODEL OF HML DYNAMICS

We now analyze the proposed model of HML in equations (6) and (9). The motor learning literature suggests that the forward learning dynamics evolve on a faster timescale than the inverse learning dynamics; see [15] for plausible neural mechanisms underlying this timescale separation. In accordance with the motor learning literature, we assume that the forward learning dynamics evolve on a faster timescale. Decomposing equations (1) and (4) into n equations (one each for cursor motion along axes), we obtain $\dot{\hat{\mathbf{x}}}_i = \hat{C}_i \hat{\mathbf{u}}$ for all $i \in \{1, \dots, n\}$. Similar expression can be written for Eq. (1). We analyze each of these equations separately, and for ease of notation we will drop the index i . Defining the slow variable $\mathbf{e}_x = (x^{\text{des}} - \mathbf{x}) \in \mathcal{E} \subseteq \mathbb{R}$, we get

$$\dot{\mathbf{e}}_x = \dot{x}^{\text{des}} - \dot{\mathbf{x}} = -C\hat{\mathbf{u}} = -W\Phi\hat{\mathbf{u}}. \quad (10)$$

Let $f_1 : \mathcal{U} \times \mathcal{E} \times \mathcal{W} \rightarrow \mathcal{E}_U$, $f_2 : \mathcal{W} \rightarrow \mathbb{R}$, $g : \mathcal{U} \times \mathcal{W} \rightarrow \mathcal{E}_W$ be defined by

$$\begin{aligned} f_1(\hat{\mathbf{u}}, \mathbf{e}_x, \hat{W}) &= -\eta \left((\hat{C}^\top \hat{C} + \mu I) \hat{\mathbf{u}} - k_P \hat{C}^\top \mathbf{e}_x \right), \\ f_2(\hat{W}) &= -W\Phi\hat{\mathbf{u}}, \\ g(\hat{\mathbf{u}}, \hat{W}) &= -\gamma \tilde{W}\Phi\delta\mathbf{u}\delta\mathbf{u}^\top\Phi^\top. \end{aligned}$$

Then the model of HML dynamics (6), (9), and (10) can be equivalently written as

$$\begin{aligned}\dot{\hat{\mathbf{u}}} &= f_1(\hat{\mathbf{u}}, e_x, \hat{W}), \\ \dot{e}_x &= f_2(\hat{W}), \\ \varepsilon \dot{\hat{W}} &= g(\hat{\mathbf{u}}, \hat{W}).\end{aligned}\quad (11)$$

Employing the change of variables $\tilde{W} = \hat{W} - W$, where W is the steady state of $\hat{W}(t)$, we get the shifted singularly perturbed system defined by

$$\begin{aligned}\dot{\hat{\mathbf{u}}} &= f_1(\hat{\mathbf{u}}, e_x, \tilde{W} + W), \\ \dot{e}_x &= f_2(\tilde{W} + W), \\ \varepsilon \dot{\tilde{W}} &= g(\hat{\mathbf{u}}, \tilde{W} + W),\end{aligned}\quad (12)$$

where we have used $\dot{\tilde{W}} = \dot{\hat{W}}$. It can be verified that $(\hat{\mathbf{u}}, e_x, \tilde{W}) = (0, 0, 0)$ is an isolated equilibrium of system (12). Moreover, the functions f_1, f_2, g are locally Lipschitz and their partial derivatives up to the second-order are bounded in their respective domains containing the origin.

A. Slower Timescale Inverse Learning Dynamics

The reduced system associated with (12) is:

$$\begin{aligned}\dot{\hat{\mathbf{u}}} &= f_1(\hat{\mathbf{u}}, e_x, W) \\ &= -\eta((\Phi^\top W^\top W \Phi + \mu I)\hat{\mathbf{u}} - k_P \Phi^\top W^\top e_x) \\ \dot{e}_x &= f_2(W) = -W \Phi \hat{\mathbf{u}}.\end{aligned}\quad (13)$$

Lemma 1 (Stability of the Reduced System): The reduced system (13) is globally asymptotically stable.

Proof: Consider the radially unbounded Lyapunov function

$$V(\hat{\mathbf{u}}, e_x) = \frac{1}{2\eta} \hat{\mathbf{u}}^\top \hat{\mathbf{u}} + \frac{k_P}{2} e_x^2.$$

The time-derivative of V along the reduced system (13) is

$$\begin{aligned}\dot{V} &= \frac{1}{\eta} \hat{\mathbf{u}}^\top \dot{\hat{\mathbf{u}}} + k_P e_x \dot{e}_x \\ &= -\hat{\mathbf{u}}^\top (\Phi^\top W^\top W \Phi + \mu I) \hat{\mathbf{u}} + k_P \hat{\mathbf{u}}^\top \Phi^\top W^\top e_x, \\ &\quad - k_P W \Phi \hat{\mathbf{u}} e_x, \\ &= -\hat{\mathbf{u}}^\top (C^\top C + \mu I) \hat{\mathbf{u}} + k_P (\hat{\mathbf{u}}^\top C^\top - C \hat{\mathbf{u}}) e_x, \\ &\leq -\alpha_1 \|\hat{\mathbf{u}}\|^2,\end{aligned}\quad (14)$$

where $\alpha_1 = \lambda_{\min}(C^\top C + \mu I) > 0$ is the smallest eigenvalue of the matrix in the argument, and $\hat{\mathbf{u}}^\top C^\top = C \hat{\mathbf{u}}$ since it is a scalar quantity. The set $S = \{(\hat{\mathbf{u}}, e_x) \mid \dot{V} = 0\}$ does not contain any trajectory of the reduced system except for $\{\hat{\mathbf{u}}, e_x\} = 0$. Hence, using LaSalle's invariance principle, the reduced system (13) is globally asymptotically stable. ■

B. Faster Timescale Forward Learning Dynamics

The boundary-layer system associated with (12) is defined using the fast timescale $\tau = t/\varepsilon$ by

$$\frac{d\tilde{W}}{d\tau} = g(\hat{\mathbf{u}}, \tilde{W} + W),\quad (15)$$

where the slow-varying states $\hat{\mathbf{u}}$ and e_x are considered frozen.

Definition 1 (Persistently Exciting Signal): A signal vector $\omega(t)$ is persistently exciting if there exist $\alpha_1, \alpha_2, \delta > 0$ such that

$$\alpha_2 I \geq \int_{t_0}^{t_0+\delta} \omega(\tau) \omega(\tau)^\top d\tau \geq \alpha_1 I, \text{ for all } t_0 \geq 0.$$

Assumption 1 (Properties of the Input): $\delta \mathbf{u}$ and its derivative $\delta \dot{\mathbf{u}}$ are bounded, i.e., $\delta \mathbf{u}, \delta \dot{\mathbf{u}} \in \mathcal{L}_\infty$, and $\delta \mathbf{u}$ is persistently exciting.

To ensure that $\delta \mathbf{u}$ is persistently exciting, a noise (ξ) is added to the inverse dynamics (9) giving

$$\dot{\hat{\mathbf{u}}} = -\eta \left((\Phi^\top \hat{W}^\top \hat{W} \Phi + \mu I) \hat{\mathbf{u}} - k_P \Phi^\top \hat{W}^\top e_x + \xi \right),$$

where $\alpha_2 T \geq \int_{t_0}^{t_0+T} \xi(\tau) \xi(\tau)^\top d\tau \geq \alpha_1 T$, for all $t_0 \geq 0$, and some $\alpha_1, \alpha_2, T > 0$.

Remark 1: Since $\delta \mathbf{u}$ is the filtered finger joints velocities, it is reasonable to assume $\delta \mathbf{u}$ and its derivative to be bounded. Additionally, since humans use exploratory noise for motor learning [13], assuming $\delta \mathbf{u}$ to be persistently exciting is also reasonable.

Lemma 2 (Stability of the Boundary Layer System):

Under Assumption 1, the boundary layer system (15) is globally exponentially stable. Therefore, the parameter estimation matrix $\hat{W}(t)$ exponentially converges to the actual parameter matrix W .

Proof: This lemma can be established using standard techniques in adaptive control [21]. For completeness, we provide an outline of the proof. Upon substituting the isolated root of \hat{W} in (15), we get

$$\frac{d\tilde{W}}{d\tau} = \varepsilon \dot{\tilde{W}} - \varepsilon \dot{W} = -\gamma \tilde{W} \Phi \delta \mathbf{u} \delta \mathbf{u}^\top \Phi^\top.$$

Consider the radially unbounded Lyapunov function

$$V_b(\hat{\mathbf{u}}, \tilde{W}) = \frac{1}{2\gamma} \tilde{W} \tilde{W}^\top.$$

The time-derivative of V_b along the boundary layer system (15) is

$$\dot{V}_b = \frac{1}{\gamma} \dot{\tilde{W}} \tilde{W}^\top = -\tilde{W} \Phi \delta \mathbf{u} \delta \mathbf{u}^\top \Phi^\top \tilde{W}^\top = -\epsilon^2 \leq 0. \quad (16)$$

Since V_b is a non-negative and non-increasing function of time, $\lim_{t \rightarrow \infty} V_b = V_b(\infty)$ exists. Eq. (16) implies $\epsilon \in \mathcal{L}_2$. Additionally, if $\delta \mathbf{u} \in \mathcal{L}_\infty$. Thus, using Barbalat's Lemma $\epsilon(t) \rightarrow 0$ as $t \rightarrow \infty$, $\lim_{t \rightarrow \infty} \dot{\tilde{W}}(t) = \lim_{t \rightarrow \infty} \hat{W}(t) = 0$.

Further, since $\delta \mathbf{u}$ is persistently exciting, it can be shown [17, Theorem 2.5.1] that $\hat{W}(t) \rightarrow W$ exponentially, and the boundary layer system (15) exponentially converges to origin. ■

C. Coupled Forward-Inverse Motor Learning Dynamics

We now present the main result of the analysis showing the stability and convergence of our proposed HML model.

Theorem 1 (Stability of the HML Model (11)): For $\varepsilon \in (0, \varepsilon^*)$, for ε^* sufficiently small, and under Assumption 1, the origin of the HML model (11) is asymptotically stable.

Proof: Specializing [22, Theorem 11.3] to the autonomous system (12), and using Lemmas 1 and 2, we can show that the origin of (11) is an asymptotically stable equilibrium for a sufficiently small ε^* . ■

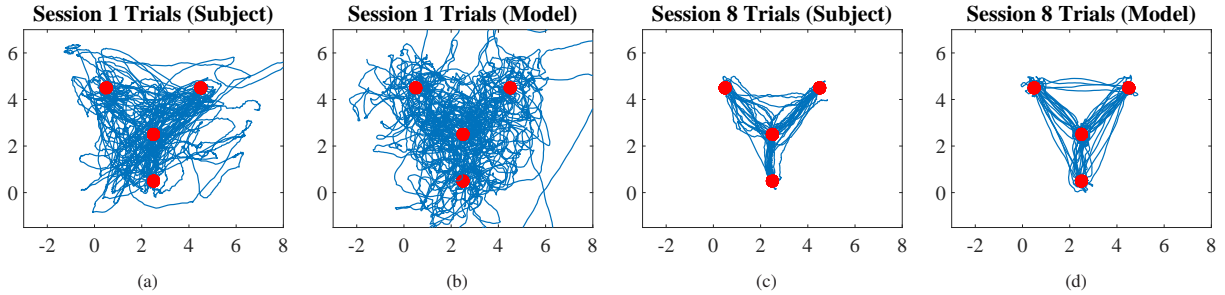


Fig. 2: **Cursor Trajectories:** Cursor trajectory data from human experiments and the fitted model.

V. MODEL FITTING AND COMPARISON WITH EXPERIMENTAL DATA

In this section, we discuss the methods used to design the HMI mapping matrix and finding the model parameters by fitting data from human subject experiments. We then show the performance of our proposed HML model by comparing it with the experimental data.

A. Designing the Forward HMI Mapping Matrix

To design the forward HMI mapping matrix, Ranganathan *et al.* [23] collected hand posture data during a *free finger exploration* phase, in which subjects freely chose arbitrary hand postures per their own discretion. They performed Principal Component Analysis (PCA) on the collected hand posture data. The first two principal components accounted for more than 80% of the variance in the joint movement data and were used in the mapping matrix C to map hand finger joints movements to cursor movement in x and y direction. In order to reduce the dimension of the learning space, we construct a synergy matrix Φ using the first four principal components from the above PCA.

B. Fitting HML Model to Experimental Data

We refer to the Euclidean norm of the cursor position at the end of movement and the target point as Reaching Error (RE). End of movement was defined as the time when the cursor reaches inside a 0.15 units radius circle of the target or after 2 seconds of the start of the movement, whichever is earlier. It can be numerically verified that for the HML model, RE follows an exponential trend with the rate of convergence η . Therefore, for the experimental data, RE was computed by averaging over similar trials (trials with same start and end points) across sessions, followed by smoothing out by moving window averaging taking a window of 10 trials. The learning rate η in the inverse learning dynamics (9) was determined by fitting RE as an exponential function of trials (k), i.e., $RE = a \exp(-\eta k) + c$. For our experimental data, the estimate of η is 0.04522 with the goodness-of-fit parameter $R^2 = 0.9019$. With the estimated inverse learning rate, we selected the forward learning rate γ as a minimizer of the norm of the difference between finger joint trajectories from human data and the model. To this end, we performed a grid search over $\gamma \in [0, 10]$. The optimum value of γ was found to be equal to 0.262, which is used to compare the HML model with the experimental data in the next section.

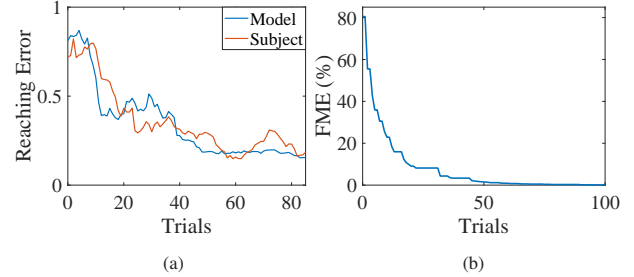


Fig. 3: **Performance Measures:** (a) RE for the subject (red) and for the fitted model (blue) as a function of trials. (b) Evolution of FME for the subject as a function of trials, only the first 100 trials are shown.

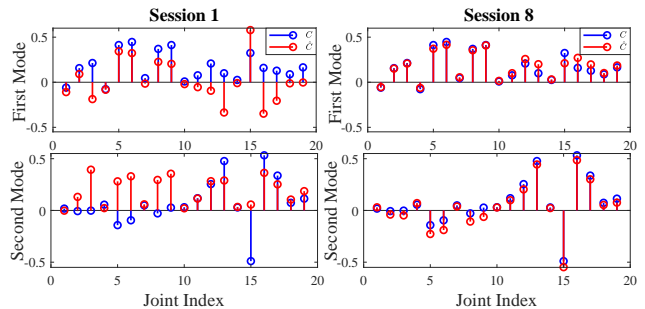


Fig. 4: **Modes of Mapping Matrix:** Evolution of SVD modes of the forward mapping matrix from Session 1 to Session 8.

C. Performance Measures: Comparing with Human Hand Data

We simulated HML model with the parameters estimated above. The model was simulated at 100 Hz, while the data glove samples finger joint positions at 50 Hz. Therefore, the trajectory data from the simulation model was sub-sampled at the same time indices as the human data for a direct comparison. We use Forward Model Error (FME) [13] to quantify the convergence of the subject's estimate of forward mapping ($\hat{C} = \hat{W}\Phi$) to the actual forward mapping matrix ($C = W\Phi$), which is defined by

$$FME_k = \frac{\|C - \hat{C}\|}{\|C\|} = \frac{\|W - \hat{W}\|}{\|W\|}$$

Fig. 2 compares the actual trajectories obtained from the human data with that coming out of our proposed model. Results show that our model can mimic the motor learning of human hand motions very closely. Noisy trajectories in

the beginning are due to high exploration noise in the initial trials; they look straighter as the trials progress and the subject/model learns the mapping. The evolution of both FME and RE with the trials is shown in Fig. 3. Both FME and RE decrease with trials and the behavior of the fitted model is consistent with the experimental data. Fig. 4 compares the SVD modes of learned forward mapping \hat{C} with the SVD modes of actual mapping matrix C . Results show that the modes of learned mapping are more consistent with that of the actual mapping matrix for the later sessions, and thus \hat{C} converges to C with high accuracy.

VI. CONCLUSION AND FUTURE DIRECTIONS

In this paper, we proposed an HML model that can mimic human motor learning in high-dimensional spaces. We leveraged the low-dimensional key motor synergies that drive the high-dimensional human finger joints movements and built up on the internal model theory of motor control to obtain a mathematical model of motor learning. We then used singular perturbation theory to establish that the proposed model of learning dynamics is asymptotically stable. We further established the conditions under which human estimate of forward mapping converges to actual forward mapping. We discussed techniques to fit the proposed model to the experimental data and showed that the model captures experimental behavior well.

This model can be leveraged for model based investigation of motor rehabilitation and designing strategies for effective motor learning assistance. For example, the HML model can be leveraged for optimal scheduling of motor rehabilitation training. The HML model could potentially help in designing a bi-directional human-robot learning framework that would allow the adaptation of rehabilitation strategies to subject-specific needs and requirements. Furthermore, robotic rehabilitation for high-dimensional motor systems has gained prominence [24], [25], [26], [27], [28], and we believe that the HML model developed in this paper can be used with such rehabilitation systems to enable bi-directional human-robot interaction.

REFERENCES

- [1] D. Mozaffarian, E. J. Benjamin, A. S. Go, D. K. Arnett, M. J. Blaha, M. Cushman, S. De Ferranti, J.-P. Després, H. J. Fullerton, V. J. Howard *et al.*, “Heart disease and stroke statistics - 2015 update: A report from the American Heart Association,” *Circulation*, vol. 131, no. 4, pp. 434–441, 2015.
- [2] J. G. Broeks, G. Lankhorst, K. Rumping, and A. Prevo, “The long-term outcome of arm function after stroke: Results of a follow-up study,” *Disability and Rehabilitation*, vol. 21, no. 8, pp. 357–364, 1999.
- [3] E. S. Lawrence, C. Coshall, R. Dundas, J. Stewart, A. G. Rudd, R. Howard, and C. D. Wolfe, “Estimates of the prevalence of acute stroke impairments and disability in a multiethnic population,” *Stroke*, vol. 32, no. 6, pp. 1279–1284, 2001.
- [4] E. Cruz, H. Waldinger, and D. Kamper, “Kinetic and kinematic workspaces of the index finger following stroke,” *Brain*, vol. 128, no. 5, pp. 1112–1121, 2005.
- [5] C. E. Lang and M. H. Schieber, “Differential impairment of individuated finger movements in humans after damage to the motor cortex or the corticospinal tract,” *Journal of Neurophysiology*, vol. 90, no. 2, pp. 1160–1170, 2003.
- [6] S. Li, M. L. Latash, G. H. Yue, V. Siemionow, and V. Sahgal, “The effects of stroke and age on finger interaction in multi-finger force production tasks,” *Clinical Neurophysiology*, vol. 114, no. 9, pp. 1646–1655, 2003.
- [7] S.-H. Zhou, J. Fong, V. Crocher, Y. Tan, D. Oetomo, and I. Mareels, “Learning control in robot-assisted rehabilitation of motor skills—a review,” *Journal of Control and Decision*, vol. 3, no. 1, pp. 19–43, 2016.
- [8] M. C. Tresch, V. C. Cheung, and A. d’Avella, “Matrix factorization algorithms for the identification of muscle synergies: Evaluation on simulated and experimental data sets,” *Journal of Neurophysiology*, vol. 95, no. 4, pp. 2199–2212, 2006.
- [9] M. Santello, M. Flanders, and J. F. Soechting, “Postural hand synergies for tool use,” *Journal of Neuroscience*, vol. 18, no. 23, pp. 10105–10115, 1998.
- [10] A. M. Haith and J. W. Krakauer, “Model-based and model-free mechanisms of human motor learning,” in *Progress in Motor Control*. Springer, 2013, pp. 1–21.
- [11] R. Shadmehr and F. A. Mussa-Ivaldi, “Adaptive representation of dynamics during learning of a motor task,” *Journal of Neuroscience*, vol. 14, no. 5, pp. 3208–3224, 1994.
- [12] S.-H. Zhou, D. Oetomo, Y. Tan, E. Burdet, and I. Mareels, “Human motor learning through iterative model reference adaptive control,” in *Proc. of IFAC World Congress*, 2011, pp. 2883–2888.
- [13] C. Pierella, M. Casadio, F. A. Mussa-Ivaldi, and S. A. Solla, “The dynamics of motor learning through the formation of internal models,” *PLoS Computational Biology*, vol. 15, no. 12, p. e1007118, 2019.
- [14] R. Shadmehr, M. A. Smith, and J. W. Krakauer, “Error correction, sensory prediction, and adaptation in motor control,” *Annual review of neuroscience*, vol. 33, pp. 89–108, 2010.
- [15] F. Yavari, F. Towhidkhah, and M. A. Ahmadi-Pajouh, “Are fast/slow process in motor adaptation and forward/inverse internal model two sides of the same coin?” *Medical Hypotheses*, vol. 81, no. 4, pp. 592–600, 2013.
- [16] K. M. Mosier, R. A. Scheidt, S. Acosta, and F. A. Mussa-Ivaldi, “Remapping hand movements in a novel geometrical environment,” *Journal of Neurophysiology*, vol. 94, no. 6, pp. 4362–4372, 2005.
- [17] S. Sastry and M. Bodson, *Adaptive Control: Stability, Convergence and Robustness*. Courier Corporation, 2011.
- [18] R. Vinjamuri, V. Patel, M. Powell, Z.-H. Mao, and N. Crone, “Candidates for synergies: linear discriminants versus principal components,” *Computational Intelligence and Neuroscience*, vol. 2014, 2014.
- [19] X. Liu and R. A. Scheidt, “Contributions of online visual feedback to the learning and generalization of novel finger coordination patterns,” *Journal of Neurophysiology*, vol. 99, no. 5, pp. 2546–2557, 2008.
- [20] D. J. Herzfeld, P. A. Vaswani, M. K. Marko, and R. Shadmehr, “A memory of errors in sensorimotor learning,” *Science*, vol. 345, no. 6202, pp. 1349–1353, 2014.
- [21] P. A. Ioannou and J. Sun, *Robust Adaptive Control*. Courier Corporation, 2012.
- [22] H. K. Khalil, *Nonlinear Systems*, 3rd ed. Prentice Hall, 2002.
- [23] R. Ranganathan, A. Adewuyi, and F. A. Mussa-Ivaldi, “Learning to be lazy: Exploiting redundancy in a novel task to minimize movement-related effort,” *Journal of Neuroscience*, vol. 33, no. 7, pp. 2754–2760, 2013.
- [24] A. Rashid and O. Hasan, “Wearable technologies for hand joints monitoring for rehabilitation: A survey,” *Microelectronics Journal*, vol. 88, pp. 173–183, 2019.
- [25] F. Zhang, L. Hua, Y. Fu, H. Chen, and S. Wang, “Design and development of a hand exoskeleton for rehabilitation of hand injuries,” *Mechanism and Machine Theory*, vol. 73, pp. 103–116, 2014.
- [26] J. C. Castiblanco, I. F. Mondragon, C. Alvarado-Rojas, and J. D. Colorado, “Assist-as-needed exoskeleton for hand joint rehabilitation based on muscle effort detection,” *Sensors*, vol. 21, no. 13, p. 4372, 2021.
- [27] P. Agarwal and A. D. Deshpande, “Subject-specific assist-as-needed controllers for a hand exoskeleton for rehabilitation,” *IEEE Robotics and Automation Letters*, vol. 3, no. 1, pp. 508–515, 2017.
- [28] ———, “A framework for adaptation of training task, assistance and feedback for optimizing motor (re)-learning with a robotic exoskeleton,” *IEEE Robotics and Automation Letters*, vol. 4, no. 2, pp. 808–815, 2019.